Poly(adipic acid-hexamethylene diamine)-functionalized multi-walled carbon nanotube nanocomposites

Xing-xiang Zhang · Qing-jie Meng · Xue-chen Wang · Shi-he Bai

Abstract Poly(adipic acid-hexamethylene diamine) (PA66)-functionalized multi-walled carbon nanotubes (PACNT) were fabricated using amino multi-walled carbon nanotubes (AMWNT), adipic acid-hexamethylene diamine salt as reactants at 260–270 °C. The solubility of AMWNT in formic acid is improved after PA66 functionalization. PA66 was successfully grafted onto the surface of AMWNT to form a core–shell nanostructure. AMWNT are surrounded by PA66 chains with an average thickness of 3 nm. The length of PA66 chains on the surface of AMWNT decreases, with the content of AMWNT increasing. The thermal decomposition temperature of the composite is lower than that of PA66 functionalized carboxylic multi-walled carbon nanotubes. The storage modulus of PACNT containing 5 wt% AMWNT is 2.8-fold that of PA66; and it increases as the content of AMWNT increases.

Introduction

Carbon nanotube (CNT), one of the most outstanding discoveries in the chemical and materials fields, is under extensive investigation for nanostructures [1]. The elastic modulus of Single-walled Carbon Nanotubes (SWNTs) and Multi-walled Carbon Nanotubes (MWNTs) is ~ 1 TPa and $\sim 0.3–1$ TPa, respectively [2]. The strength of SWNTs and MWNTs is 50–500 GPa and 10–60 GPa, respectively [2]. The resistivity is 50–50 $\mu\Omega$ cm for both SWNTs and MWNTs [2]. The thermal conductivity is 3,000 W m^{-1} K^{-1} for both SWNTs and MWNTs which is about double that of diamond and electric-current-carrying capacity 1,000 times higher than copper wire [2]. The unique properties of CNTs make them possess wide applications, including high-strength composites [3], conducting and semi-conducting materials [4, 5], energy storage devices [6], electro-mechanical actuators, and so on. Their realistic applications in materials and devices have been hindered by their poor compatibility with matrix, however. The early CNTs' nanocomposites were prepared by physically mixing multi-walled carbon nanotubes (MWNTs) with polymers (non-covalent CNT modification) [7]. CNTs are easily drawn out from matrix due to the weak interaction between polymers and the surfaces of CNTs [8]. Several methods, for example, solution casting [9], electro-spinning [10, 11], and surfactant-assisted processing of CNTs-polymer composites [12], have been developed for the fabrications of CNTs-polymer nanocomposites to improve the interaction force between CNTs and matrix. The measured mechanical properties are still noticeably lower than the theoretical values, however. If the polymer functionalized MWNTs (polymer chains covalent chemical bonding to CNTs) were used as precursors to mix with polymer, the dispersion of CNTs in polymer and the mechanical properties of the nanocomposites would be significantly enhanced [13, 14].

PA66 is an important commercial semi-crystalline polymer. It is widely used as engineering plastic, fibers, and films, etc. The modulus of PA66 is relatively low, however. Attempts have been made to improve this property. A series of PA66/MWNT films were fabricated by mixing MWNTs and AMWNT with PA66 in formic acid, which was then poured onto glass plates [13]. After being vacuum-dried for 24 h at 80 °C, the films were subsequently compression molded between Teflon sheets at

X. Zhang (✉) · Q. Meng · X. Wang · S. Bai
Tianjin Municipal Key Lab of Fiber Modification and Functional Fibers, Institute of Functional Fibers, Tianjin Polytechnic University, Tianjin 300160, China
e-mail: zhangpolyu@gmail.com

280 °C. AMWNT are more homogeneously distributed than MWNTs in the PA66 matrix. With 0.5 wt% MWNTs in PA66, the maximum tensile stress and Young's modulus improve over the neat PA66 film by ~ 24 and 14%, respectively. However, the film containing 0.5 wt% AMWNTs show an improvement of $\sim 43\%$ in maximum tensile stress and $\sim 32\%$ in Young's modulus over pristine PA66 film. PA66-functionalized Carboxylic Multi-walled Carbon Nanotubes (CMWNTs) were fabricated at 260–270 °C by in situ polymerization in our previous research [14]. The formic acid washed and vacuum-dried composites were melt-spun into fibers. The CMWNT content (W_c) in the composite was calculated based on the residual weight of Thermogravimetric Analysis (TGA). The calculated W_c of every sample is significantly higher than that in raw material. The W_c is 3–50 times of CMWNT content in the raw material. This result implies that some of adipic acid-hexamethylene diamine salts do not react with CMWNTs. This is true especially when the CMWNT content is low. Aggregation of CMWNTs is not observed in the fracture surface of the composite fiber. The CMWNTs are not completely pulled out from the matrix, implying strong interactions as a result of functionalization. The tensile strength of the fiber containing 0.5 wt% carboxylic multi-walled carbon nanotubes is $\sim 148\%$ that of pristine PA66 fiber; meanwhile, the Young's modulus is $\sim 162\%$ that of pristine PA66 fiber. The strain of the fiber decreases as the content of CMWNT increases.

The fabrication of PA66 functionalized AMWNT composites using amino multi-walled carbon nanotubes, adipic acid-hexamethylene diamine salt as reactants have never been reported. AMWNT were melt-mixed with adipic acid-hexamethylene diamine salt and heat-treated at 260–270 °C for 2 h for the purpose of this article. The structure and properties of the PA66-functionalized Multi-walled Carbon Nanotubes were investigated. The results were compared with that of solution cast AMWNT/PA66 films and PA66 functionalized CMWNT composite fibers.

Experimental

Raw materials

CMWNT was obtained from Institute of Organic Chemistry in Chengdu of the Chinese Academy of Sciences. Adipic acid, hexamethylene diamine, thionyl chloride (SOCl$_2$), ammonium carbonate, sodium hypochlorite anhydrous alcohol, and other chemical reagents (all of them were analytic grade) were obtained from The Development Center of Chemical Agents in Tianjin. They were used without further purification.

Sample preparation

Acylation of CMWNT

One gram of CMWNT and 20 mL of SOCl$_2$ were added to a 250 mL three-necked flask immersed in a water bath. The flask was equipped with a reflux condenser. The black suspended liquid was stirred at 70 °C for 24 h. Then, excess SOCl$_2$ was removed by vacuum filtration through a 0.22 μm PTFE membrane. The products were washed with anhydrous THF until the filtrate became colorless and were subsequently vacuum dried at 50 °C for 12 h. Acylated multi-walled carbon nanotubes (MWNT-COCl) were obtained.

Amidation of MWNT-COCl

One gram MWNT-COCl and 5 g amine carbonate were added to a 250 mL three-necked flask. Fifty milliliters of ammonia were added drop-wise to the mixture, which was allowed to react at room temperature under continuous stirring for 6 h. Upon completion, the mixture was vacuum-filtered through a 0.22 μm polytetrafluoroethylene (PTFE) membrane and then washed 5 times with distilled water to remove the excess ammonia. The black solid (MWNT-CONH$_2$) was vacuum dried at 50 °C for 2 h.

Fabrication of AMWNT

One gram MWNT-CONH$_2$ was put into a 250 mL three-necked flask immersed in an icewater bath of 0–5 °C. Thirty milliliters of sodium hypochlorite were slowly added drop-wise to the flask, which was allowed to react at 0–5 °C under intensive stirring for 4 h. Then, the mixture reacted at 70 °C for 2 h under continuous stirring. MWNT-CONH$_2$ was transformed into MWNT-NH$_2$ by Hoffman degradation [15]. The product was poured onto a 0.22 μm PTFE membrane and washed 5 times with distilled water. The resultant multi-walled carbon nanotube terminated with an amino group (AMWNT), that was characterized using Raman spectra, then dried in a vacuum oven at 50 °C for 4 h.

TEM micrographs of AMWNT are shown in Fig. 1. The internal diameter of AMWNT is 5–8 nm; and the external diameter is 10–15 nm. It has approximately 10 graphite layers. AMWNT indicates the presence of some defects associated with the formation of amino groups in the open ends, sidewalls, and defect sites of CNTs.

Synthesis of PACNT

Adipic acid-hexamethylene diamine salt was fabricated as follows: 7.3 g adipic acid and 5.9 g hexamethylene
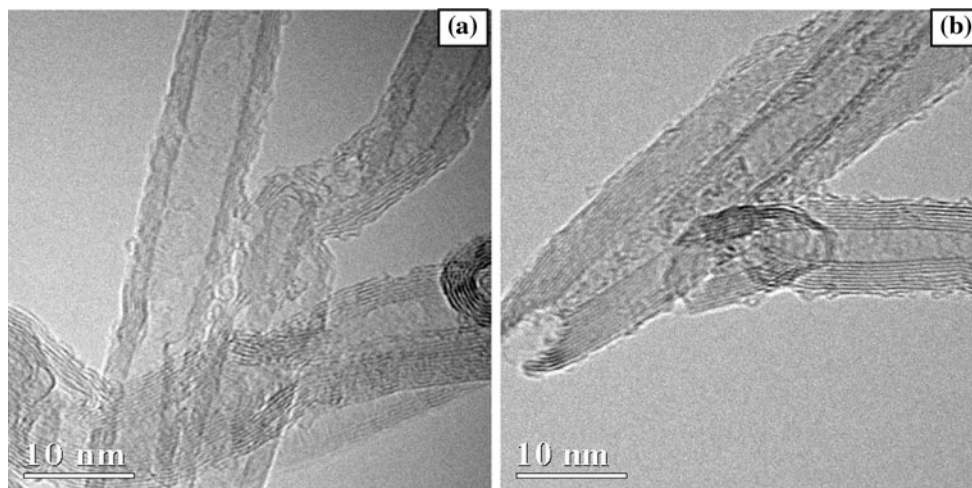
Fig. 1 TEM micrographs of **a** side surface, **b** open end of AMWNT

diamine were dissolved in 50 and 60 mL anhydrous alcohol at 70 °C, respectively. The hexamethylene diamine solution was dropped into the adipic acid solution under stirring. The white deposition was separated by filtration using a Buchner filter and washed with anhydrous alcohol. The resulting solid was dried in a vacuum oven at 50 °C.

PACNT were fabricated as follows: adipic acid-hexamethylene diamine salt and a predetermined mass of AMWNT were ground together in an agate mortar. The mixture was put into a test tube with a side pipe and compacted at the bottom of the test tube with a glass rod. A rubber tube linked to the side pipe was the outlet for the nitrogen. The other end of the rubber tube was immersed in water. Then the test tube was purged with nitrogen for 5 min to remove air before polymerization. The mixture was heated to 200–210 °C in a salt bath (sodium nitrate and potassium nitrate in a mass ratio of 1) under an atmosphere of nitrogen. The gas flow was decreased when the mixture melted. After 2 h, the temperature of the salt bath was increased to 260–270 °C and kept there for approximately 2 h. Then the test tube was cooled to room temperature. A hard block was obtained, and was crushed into small pieces and immersed in formic acid for 3 days. It was then washed 5 times in formic acid to remove unreacted monomer, oligomers, and partial PA66 that had not connected with MWNTs. The solid was separated by vacuum filtration using a 0.22 μm polytetrafluoroethylene membrane. The black solid (PACNT) was obtained after drying at 50 °C. PACNT containing different contents of AMWNT were synthesized with the same process.

The black powders were molded by hot pressure casting at 120 °C to form wafer (diameter 7 mm, thickness 2 mm). The wafers were used as the samples for dynamic mechanical analysis.
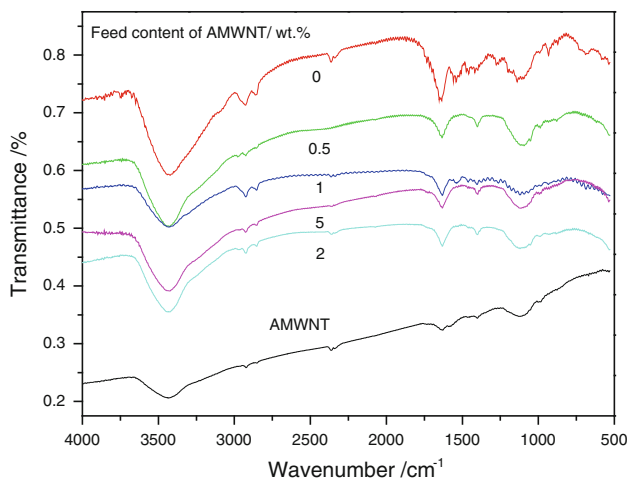
Testing procedure

Morphologies of the samples were investigated using Transmission Electronic Microscopy (TEM, Philips Tancnai F20) with a field emission source. The accelerating voltage was 20 kV. The samples were prepared by ultrasonic dispersion of PACNT in ethanol, dropping on a copper grid, and drying at room temperature. FTIR spectra of the samples were obtained with a Fourier Transform Infrared Spectroscope (FTIR, VECTOR22) using KBr disk method. The thermal stabilities in the range of 50–700 °C were measured with Thermogravimetric Analysis (TGA, NETZSCH STA409 PC/PG TG-DTA) in an atmosphere of nitrogen at a heating rate of 10 °C/min. Raman analysis of MWNTs, MWNT-COOH, MWNT-CONH$_2$, MWNT-COCl, and MWNT-NH$_2$ were carried out using a Renishaw Invia spectrometer. Green laser (514 nm) was used to excite the samples. The dynamic mechanical properties of the samples (diameter 7 mm, thickness 2 mm) were examined using a Dynamic Mechanical Analyzer (DMA, NETZSCH DMA 242) in an atmosphere of nitrogen at a heating rate of 5 °C/min and a frequency of 1 Hz. Melting and crystallization behaviors were investigated in an atmosphere of nitrogen in the range of 40–300 °C by using a Differential Scanning Calorimetry (DSC, Perkin-Elmer DSC7) at heating and cooling rates of ±10 °C/min.

Results and discussion

Formation of PACNT

FTIR spectra of AMWNT and PACNT with various contents of AMWNT are shown in Fig. 2. The broad band at 3,433 cm^{-1} in the spectrum of AMWNT is assigned to

Fig. 2 FTIR spectra of AMWNT and PACNT

Fig. 3 Photos of (1) AMWNT; (2) formic acid; (3) PA66 formic acid solution; (4) Sample No. 2; (5) Sample No. 3; (6) Sample No. 4; (7) Sample No. 5 and (8) Sample No. 6

hydrogen-bonded –NH and stretching vibrations of N–H bond. The band at 2,923 cm^{-1} is assigned to the dissymmetry stretching vibration of –CH$_2$ group in AMWNT. The bands at 1,401 and 1,128 cm^{-1} are assigned to the stretching vibration of the C–N group. With the increase of the content of AMWNT, a red shift of N–H bands between 3,423 and 3,439 cm^{-1} appears in the spectrum of PACNT. The C=O stretching vibration occurs at 1,631 and 1,635 cm^{-1} for PA66. The bands at 1,540 and 1,548 cm^{-1} are assigned to a combination of the bending vibration of the N–H bond and the stretching vibration of the C–N bond of the amide group [16]. FTIR results indicate the existence of characteristic peak of amide in PACNT.

One hundred milligrams of AMWNT and PACNT containing various contents of AMWNT were mixed with 10–14 mL formic acid. The photos of these samples are shown in Fig. 3.

Formic acid is colorless and transparent. The upper liquid of AMWNT suspension is colorless and transparent; however, AMWNT deposits at the bottom of the tube. In contrast, samples No. 2–6 are a transparent brown solution. When the content of AMWNT increases, the color of the solution becomes deeper. PACNT are soluble in formic acid. It proves that PA66 wrapped and grafted on the surface of AMWNT and improves their solubility in formic acid [17, 18].

Morphology of PACNT

Figure 4 shows TEM images of sample No. 5. It is observed that the surface of AMWNT is coated with a polymer layer. PA66 coats both the open end as well as the complex surface topography of the nanotube. PA66 is apparent on the external wall along the tube axis direction. It is found that the thickness of the polymer surface layer imaged on the kinks of the tube is slightly higher than that

on the wall. This is probably caused by more amino groups on the kink of the tube than on the tube wall. The maximum thickness is approximately 3 nm.

Thermal stability

TG and DTG plots, which are used to investigate the amount of PA66 chains grafted to AMWNT, are presented in Fig. 5. The thermal decomposition of the sample below 475 °C is primarily caused by the decomposition of PA66 chains. The onset of the decomposition temperature (T_i) and the temperature at maximum weight loss rate (T_p) were measured from the DTG curves. Both T_i and T_p decrease as the content of AMWNT increases. T_i and T_p of PACNT are significantly higher than those of PA6 functionalized SWNTs [16]. PA6 functionalized SWNTs decompose at approximately 300 °C, however, the decomposition temperature increases as the SWNT content is increased. The thermal decomposition of PA66/MWNT film, which was fabricated by mixing 0.5 or 1 wt% AMWNT with PA66 in formic acid and compression molding at 280 °C, starts at approximately 400 °C [13]. The thermal decomposition temperature of solution mixed composite is equivalent to that of PA66 functionalized AMWNT in this article. They are 15–17 °C lower than that of PA66 functionalized CMWNT [14], however. In other words, the thermal stability of PA66 functionalized CMWNT is usually higher than that of PACNT as the content of functionalized MWNT is the same. This is probably caused by more defects on amino multi-walled carbon nanotubes than on carboxylic multi-walled carbon nanotubes. One or a few
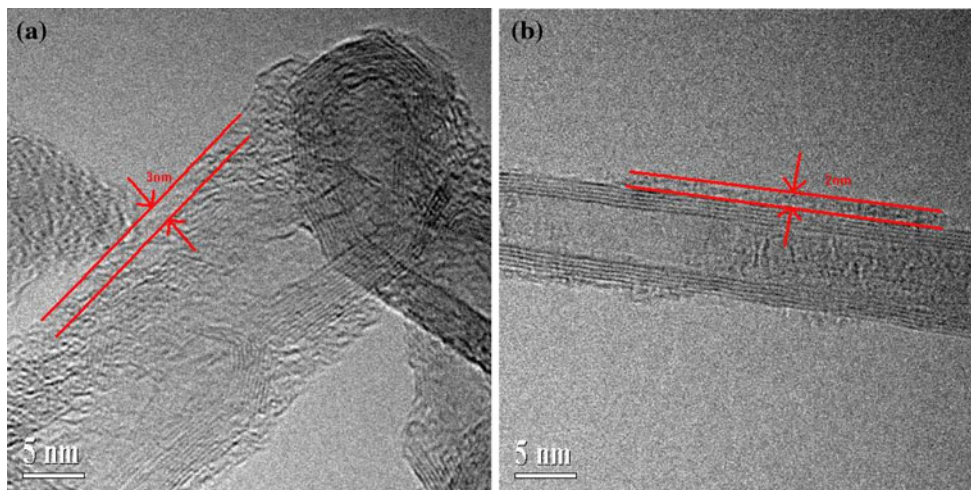
Fig. 4 TEM micrographs of PACNT

walls were destroyed in the process of acid treatment as they are shown in Fig. 1. The shifts of G bands and D bands, the ratio of G band intensity and D band intensity on Raman spectra indicate increasing deterioration of MWNTs from MWNTs to MWNT-COOH, MWNT-COCl, MWNT-CONH$_2$, and MWNT-NH$_2$. TGA results show that the thermal stability of the functionalized MWNT decreases rapidly, especially in the process of Hoffman degradation. The functionalization of MWNT surfaces causes defects on them, thus deteriorating the thermal stability of MWNTs. This deterioration of thermal stability of AMWNT is transferred to PACNT.

The weight loss of AMWNT is 12.5 wt% in the TG plot in the range of 50–700 °C. In contrast, the weight loss of MWNTs is 4.3 wt% in the same temperature range. The difference of weight loss between AMWNT and MWNTs is 8.2 wt%. The weight loss of the sample decreases, with the content of AMWNT increasing. The amino group density on AMWNT is estimated from this difference of weight loss [19]. Assuming all of the functional groups on AMWNT react with hexamethylene diamine and all of PA66 chains are grafted on AMWNT, the mean number of

average molecular weights and the number of repeating units of grafted chains are estimated [19, 20]. The results are listed in Table 1. It is noted that the increase in content of AMWNT serves to decrease the grafting chain length onto MWNTs. It is approximately 6.8 mmol per gram of AMWNT, 7.6 mmol per gram of neat CNTs, or approximately 91 functional groups per 1,000 carbons [20].

Most of the non-functional PA66 are removed by washing the mixture in formic acid, since formic acid is a solvent of PA66. Some polymers absorbed on the surfaces of MWNTs cannot be removed by washing [21]; however, the residue in this study probably contains a small portion of non-covalent PA66. MWNTs can absorb 5–50 wt% of non-functional polymer [22]. AMWNT content (W_c) in the composite was calculated based on the residual weight of TG. The calculated W_c of every sample is significantly higher than that in raw material. It is 8.2 wt% for Sample No. 3 which is ~40 times of that in the raw material. It is 15.0 wt% for Sample No. 6 which is ~3 times of that in the raw material. This result implies that some of adipic acid-hexamethylene diamine salts do not react with AMWNT. This is true especially when the AMWNT

Fig. 5 TG and DTG plots of PACNT with various contents of AMWNT. **a** TG; **b** DTG
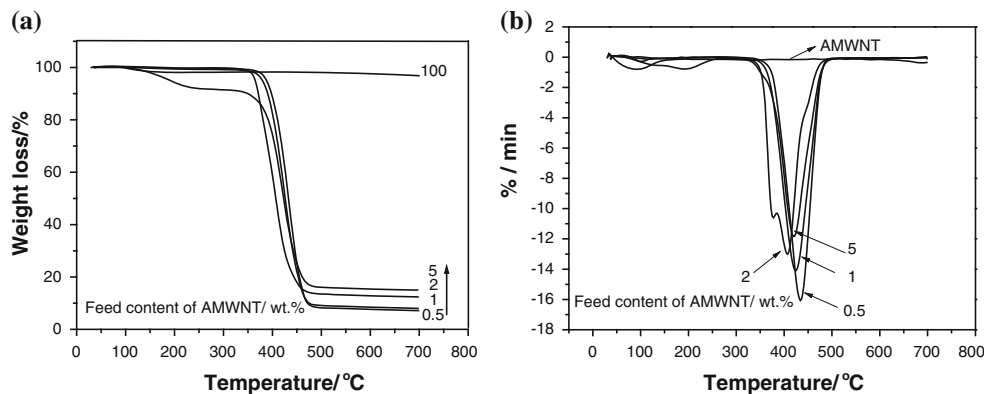
Table 1 Effect of contents of AMWNT on the weight loss and P A66 chain length

Sample No.	AMWNT/wt%	T_i/°C	T_p/°C	Weight loss[a]/wt%	Residue weight/wt%	W_c/wt%	M_p/100 g	M_h/100 g	W_p/100 g	$\overline{M}n$	d
AMWNT	100	302	340	12.5	87.5	(100)			0		
1	0	415	444	100	0	(0)			100		
2	0.1	418	448	95.3	4.7	5.0	0.41	0.037	95.0	3,090	10
3	0.5	401	434	92.8	7.2	8.2	0.68	0.062	91.8	1,480	6
4	1	392	424	92.0	8.0	9.1	0.76	0.069	90.9	1,317	5
5	2	362	407	87.6	12.4	14.2	1.18	0.107	85.8	801	3
6	5	389	420	85.0	15.0	17.1	1.43	0.130	82.9	637	2

[a] Weight loss of PACNT by TG; W_c—AMWNT content in PACNT = (residue weight of sample No n—residue weight of AMWNT)/residue weight of AMWNT; M_p—Mole of carbon atoms in PACNT = W_c/12.0 (mass of carbon atom); M_h—Mole of amino groups in PACNT = $M_p \times 9.1\%$ (ratio of amino groups on all of the carbon atoms of AMWNT); W_p—PA66 content in PACNT; $\overline{M}n = W_p/M_h$; $d = \overline{M}n/226$ [molecular weight of amide repeating unit].

content is low. The calculated PA66 molecular chain lengths attached to MWNTs are valuable since the ratio of non-functional PA66 is low. The estimated maximum content of non-functional PA66 is 7.5 wt% for Sample No. 6; and it is 4.1 wt% for Sample No. 3.

Melting and crystallization

DSC heating and cooling behaviors of PACNT with various feed contents of AMWNT are shown in Fig. 6. Twin melting peaks are observed on the DSC heating curves of all the samples with or without AMWNT, marked as $T_{m,1}$ (peak at low temperature) and $T_{m,2}$ (peak at high temperature). The melting temperature of PACNT increases and the crystallization temperature decreases when AMWNT is added. Multiple peaks on the heating scan were observed and discussed before for both pristine PA66 [23, 24] and PA66/MWNTs composites [13, 25]. $T_{m,1}$ is generally attributed to the melting of the thin lamellae formed during cooling and $T_{m,2}$ is attributed to the melting of the thickened crystals during the heating/annealing process [23–25]. The samples in this article were fabricated using AMWNT and adipic acid-hexamethylene diamine salt as reactants, which are different from those fabricated by mixing MWNT-COOH or MWNT-NH$_2$ with PA66 pellets [13, 25]. The molecular weight of PA66 is high and constant in the latter; however, the chain length of PA66 linked on MWNTs is short in the former. As a result, both $T_{m,1}$ and $T_{m,2}$ decrease when AMWNT is added. This can be explained as the molecular weight dependence of equilibrium melting temperature. As the content of AMWNT increases, the number of amino groups on the MWNTs is increased; meanwhile, the number average molecular weight of the PA66 chain grafted on MWNTs decreases from 1,480 to 637 (Table 1).

The crystallization temperature shifts to lower temperature when AMWNT is added (Fig. 6b). This phenomenon has been observed and discussed in PA66/MWNTs nanocomposites [25]. Both nucleation effect and confinement of MWNT network affect the crystallizing behavior: similar onset temperatures indicate that non-isothermal crystallization of PA66 starting at similar temperature, however, MWNT network imposes a confinement effect on PA66 chain diffusion and crystal growth [25]. This confinement of MWNT network slows down the crystallization process, which lead to lower crystallization temperatures for the nanocomposites. In contrast, the crystallization temperature of solution cast film increases marginally with the introduction of the amino MWNTs, indicating that nanotubes nucleate crystallization [13]. The confinement and restriction of usual MWNTs to PA66 chains also leads the crystallization temperature shift to lower temperature [13]. In the present case, both the decrease of chain length of PA66 and confinement of functionalized MWNTs has a more noticeable effect on the crystallization temperature than the nucleation effect of MWNTs. The crystallizing temperature shifts to lower temperature when AMWNT is added in the nonocomposite.

Dynamic mechanical properties

Figure 7 shows the storage modulus and loss factor curves of PACNT wafers on 1 Hz. The corresponding data are listed in Table 2.

The storage modulus of PACNT wafer below 70 °C increases, with the content of AMWNT increasing. The storage modulus at 25 °C increases from approximately 36 MPa for pure PA66 to approximately 100 MPa for the sample containing 5 wt% AMWNT. It is 2.8-fold that of control. The reinforcement of AMWNT to the storage
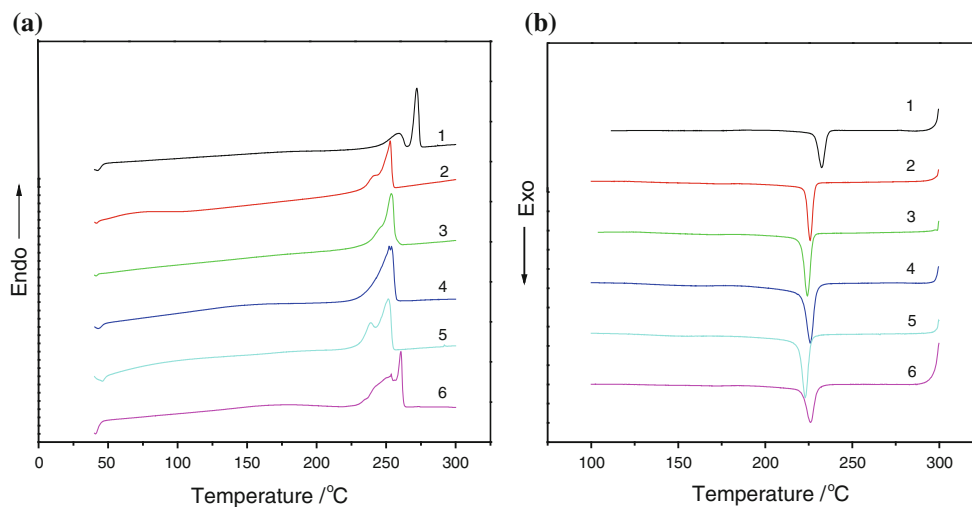
Fig. 6 DSC **a** heating and **b** cooling curves of PACNT with various feed contents of AMWNT
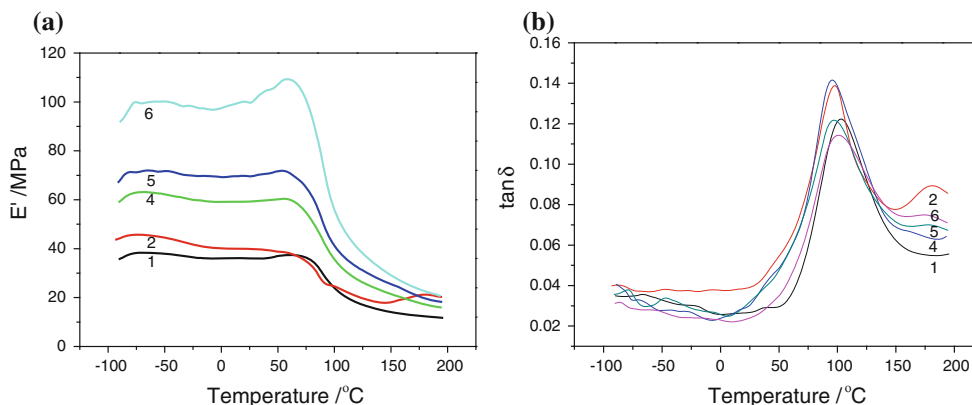

Fig. 7 Storage modulus of PACNT (1 Hz). **a** Storage modulus; **b** Loss factor

Table 2 Effect of content of AMWNT on storage modulus

Sample No.	1	2	4	5	6
AMWNT/wt%	0	0.1	1	2	5
E'/MPa (25 °C)	36	40	59	70	100
T_g/°C	103.2	98.1	96.0	97.2	100.1

modulus is associated with PA66 grafts, which are compatible with PA66 chains. These PA66 chains can physically knot and tangle together with polymer chains in the matrix. AMWNT serves as the network centers to transfer local stress evenly to all other polymer chains. The mechanical properties of PACNT are improved. The reinforcing effects of AMWNT on PA66 matrixes are higher than those on PEO matrix [26].

The glass transition temperatures (T_g, peak temperature on Tanδ-temperature curve) of PA66 and PACNT are affected by the AMWNT contents. T_g decreases from approximately 103 to 96 °C as the AMWNT content increases from 0 wt% (control) to 1 wt%. This can be understood as the decrease of the PA66 molecular chain length linked to MWNT, with an increase of the chain tail. T_g increases from 96 to 100 °C as AMWNT content increases from 1 to 5 wt%. It is well known that in polymer matrix composites, the T_g of the polymer matrix depends on the free volume of the polymer, which is related to the affinity between the filler and the polymer matrix [27]. A stronger interfacial adhesion between diamine-modified MWNTs and PA6 matrix was observed when it was compared with that of MWNTs and PA6 matrix. It decreases the free volume and shifts the T_g to higher temperature as the content of diamine-modified MWNTs increases [28]. Both the decrease of the PA66 molecular chain length linked to MWNT and the increasing interfacial adhesion between AMWNT and PA66 matrix affect the T_g of the nanocomposite as AMWNT content increases. The latter is prominent as AMWNT content exceeds 1 wt%.

Conclusions

PA66 was successfully grafted onto the surface of amino multi-walled carbon nanotubes to form a core–shell nanostructure. The dissolubility of AMWNT in formic acid is improved by PA66 grafting. Amino multi-walled carbon nanotubes are coated by PA66 chains with average thickness of approximately 3 nm. The length of PA66 chains on the surface of AMWNT decreases, with the content of AMWNT increasing. The thermal decomposition temperature of the composite is lower than that of PA66 functionalized carboxylic multi-walled carbon nanotubes. The storage modulus of PACNT containing 5 wt% AMWNT is 2.8-fold that of PA66; and it increases as the content of AMWNT increases.

References

1. Iijima S (1991) Nature 354(6348):56
2. Xie XL, Mai YW, Zhou XP (2005) Mat Sci Eng R49:89
3. Tang WZ, Santare MH, Advani SG (2003) Carbon 41(14):2779
4. Berger C, Yi Y, Wang ZL et al (2002) Appl Phys A 74(3):363
5. Berger C, Poncharal P, Yi Y et al (2003) J Nanosci Nanotech 3(1–2):171
6. Dillon AC, Heben M (2001) J Appl Phys A 72(2):133
7. Haggenmueller R, Zhou W, Fischer JE et al (2003) J Nanosci Nanotech 3(1):105
8. Frankland SJV, Caglar A, Brenner DW et al (2002) J Phys Chem B 106:3046
9. Muňoz E, Dalton AB, Collins S et al (2004) Adv Eng Mater 6(10):801
10. Frank K, Gogotsi Y, Ashraf A et al (2003) Adv Mater 15(14):1161
11. Sreekumar TV, Liu T, Kumar S (2003) Chem Mater 15(1):175
12. Mottaghitalab V, Spinks GM, Wallace GG (2005) Synth Met 152(1–3):77
13. Sengupta R, Ganguly A, Sabharwal S et al (2007) J Mater Sci 42(3):923. doi:10.1007/s10853-006-0011-1
14. Meng QJ, Wang ZM, Zhang XX, et al. (2010) High Perform Polym. doi:10.1177/0954008309341919
15. Hu ZY, Zhang SF, Yang JZ et al (2003) J Appl Polym Sci 89:3889
16. Gao JB, Itkis ME, Yu AP et al (2005) J Am Chem Soc 127(11):3847
17. Yang YK, Xie XL, Wu JG (2006) J Polym Sci A 44(12):3869
18. Yang YK, Xie XL, Wu JG et al (2006) Macromol Rapid Commu 27(19):1695
19. Meng QJ, Zhang XX, Bai SH (2007) J Appl Polym Sci 106(3):2018
20. Kong H, Gao C, Yan DY (2004) J Am Chem Soc 126(2):412
21. Baskaran D, Mays JW, Bratcher MS (2005) Polymer 46(14):5050
22. Baskaran D, Mays JW, Bratcher MS (2005) Chem Mater 17(13):3389
23. Mitomo H, Nakazato K, Kuriyama I (2003) Polymer 19:1427
24. Dreyfuss P, Keller A (1970) J Polym Sci B 8:253
25. Li LY, Li CY, Ni CY et al (2007) Polymer 48:3452
26. Jia ZJ, Wang ZY, Xu CL et al (1999) Mater Sci Eng A 271(1–2):395
27. Yuen SM, Ma CM, Lin YY et al (2007) Compos Sci Technol 67(11–12):2564
28. Meng H, Sui GX, Fang PF et al (2008) Polymer 49:610